New exact plasma equilibria with axial and helical symmetry ⊘

Jason M. Keller; Alexei F. Cheviakov ✉ iD

Check for updates

View Online   Export Citation   CrossMark

New exact plasma equilibria with axial and helical symmetry

View Online   Export Citation   CrossMark

Jason M. Keller[a)] and Alexei F. Cheviakov[b)] [iD]

AFFILIATIONS

Department of Mathematics and Statistics, University of Saskatchewan, Saskatoon, Saskatchewan S7N 5E6, Canada

[a)]Electronic mail: jmk810@mail.usask.ca
[b)]Author to whom correspondence should be addressed: shevyakov@math.usask.ca

ABSTRACT

We derive new exact closed-form solutions of magnetohydrodynamics equations, with and without dynamics, which model astrophysical jets and other prolonged plasma configurations. The solutions are obtained in static and dynamic incompressible equilibrium settings, in axial and helical symmetry assumptions, and are given in terms of Whittaker, Coulomb, and Heun special functions. For each symmetry, two distinct families of physical solutions arise, corresponding to two distinct pressure profiles. One pressure profile models plasmas supported by an external pressure and is suitable for the description of plasma configurations in a medium, such as atmosphere. The second profile features higher pressure inside the plasma domain and can model plasmas residing in a vacuum. Examples of static and dynamic solutions in axially and helically symmetric settings, including solutions with boundary current sheets, are presented and discussed.

Published under an exclusive license by AIP Publishing. https://doi.org/10.1063/5.0165963

I. INTRODUCTION

The system of incompressible magnetohydrodynamics (MHD) equations

$$\frac{\partial \rho}{\partial t} + \text{div } \rho \mathbf{V} = 0, \tag{1.1a}$$

$$\rho \frac{\partial \mathbf{V}}{\partial t} = \rho \mathbf{V} \times \text{curl } \mathbf{V} - \frac{1}{\mu} \mathbf{B} \times \text{curl } \mathbf{B} - \text{grad } P - \rho \text{ grad} \frac{|\mathbf{V}|^2}{2}, \tag{1.1b}$$

$$\frac{\partial \mathbf{B}}{\partial t} = \text{curl}(\mathbf{V} \times \mathbf{B}), \tag{1.1c}$$

$$\text{div } \mathbf{B} = 0, \quad \text{div } \mathbf{V} = 0, \tag{1.1d}$$

and specifically, its incompressible equilibrium reduction, have been broadly used in mathematical modeling of plasmas that occur as natural phenomena and in laboratory settings, including Earth magnetosheath, star formation environments, astrophysical jets, and plasma confinement devices. In (1.1), ρ denotes the plasma density, $\mathbf{B}$ is the magnetic induction vector, $\mathbf{V}$ is the plasma velocity vector, P is the scalar pressure, and μ is the magnetic permeability coefficient. More general continuum plasma models take into account essential time dependence, external forcing, more general equations of state, anisotropy, nonzero resistivity and/or viscosity, and further physical effects (see, e.g., Refs. 1 and 2 and references therein).

In this work, we are interested in exact solutions of the partial differential equations (PDEs) (1.1) in applications to astrophysical jet modeling. Jets are highly collimated streams of plasma that have been observed in a variety of settings in radio, optical, X- and γ-ray bands. Astrophysical jets are associated with active galactic nuclei, young stellar objects, neutron stars and black holes, as well as some pulsars and microquasars.[3,4] Well known examples include jets emitted by the supergiant elliptical galaxy Messier 87 and the starburst galaxy Centaurus A, in which plasma jets extend over $\sim 5 \times 10^3$ and $\sim 10^6$ light years, respectively.[5,6] Common models of astrophysical jet formation by supermassive black holes are based on accretion of matter onto the black hole and electrodynamic processes fueled by black hole's rotation energy. In a typical setting, twin opposite plasma jets are emitted in the direction perpendicular to the accretion disk (see Refs. 3 and 7 and references therein). Astrophysical jets propagate in a vacuum or in an ambient matter, such as previously ejected gas shells or interstellar and intergalactic gas. In some cases, such as the jet in Messier 87, plasma pressure within the jet can exceed ambient pressure, while in pressure confinement models, the opposite might be possible.[3]

A natural approach to a simplified model of an astrophysical jet is the assumption of a dynamic equilibrium $\partial/\partial t \equiv 0$, and further, an axial symmetry, as has been done for example in Ref. 8. However, many of the observed jets (such as, for example, the jet in Messier 87) do not appear axially symmetric, but rather exhibit an approximate

06 February 2024 19:55:52

helical symmetry (Ref. 9 and references therein). Helical symmetry can be imposed as a coordinate reduction in the helical coordinate system.[10] Helical coordinates are a non-orthogonal coordinate triple related to cylindrical coordinates, with coordinate curves defined by straight lines in the z-direction and two families of opposite helices wound on a given cylinder with a fixed radius. Helical symmetry implies the independence of physical fields of one of the helical coordinates, or in other words, the invariance of a configuration with respect to a simultaneous z-translation and rotation around the z-axis. Helical coordinates and helically invariant solutions have recently been playing an increasingly prominent role in continuum mechanics. Approximately helically invariant flows have been observed in a variety of physical settings, including combustion, propeller and wing rip vortices in fluids and gases, blood flows, free surface flows from rotating nozzles, instability modes in laminar and turbulent swirl flows, and plasma-related contexts, such as plasma discharges and plasma confinement models (see, e.g., Refs. 11–20). Similar to axially symmetric reductions, helically symmetric PDE systems can admit additional structure, such as additional symmetry groups and conserved quantities.[21–23] Time-dependent helical coordinates have been introduced.[24]

In the axially or helically symmetric assumption, static MHD equilibrium equations reduce to a single scalar PDE: the Grad–Shafranov (Bragg–Hawthorne) and the Johnson–Frieman–Kulsrud–Oberman (JFKO) equation, respectively.[25–28] Linear instances of these equations have been used to obtain explicit infinite-parameter axially and helically symmetric plasma equilibrium solutions.[8,9,29,30] Such solutions provide physically relevant models of astrophysical jets stretched along the cylindrical axis. Lower pressure values near the axis corresponds to models of jets propagating in an ambient medium; the plasma velocity and the magnetic field in these solutions decrease exponentially in terms of the cylindrical radius.

In this work, we present and analyze new exact steady and unsteady MHD equilibria in both axially and helically symmetric settings. In each setting, two families of solutions are derived: one family corresponds to a jet model in an ambient medium and generalizes the solutions in Refs. 8 and 9 the other family features higher plasma pressure values on the jet axis and models jets in a vacuum. The new solutions are also given by closed-form expressions, allow for superposition, and can be chosen to behave periodically or non-periodically along the jet axis.

The paper is organized as follows. In Sec. II, we briefly review the physical requirements on solutions of the full MHD system as well as and its axially and helically symmetric reductions. Section III is concerned with axially symmetric solutions. Such solutions are constructed from the Grad–Shafranov PDE and correspond to two different types of pressure profiles, the first with a higher pressure at the boundary of the plasma domain, with the radial part written in terms of Whittaker functions, and the second with a higher pressure in the center of the plasma jet, with radial dependence in terms of Coulomb wave functions. Examples of exact solutions satisfying natural physical requirements are presented for both solution families. In Sec. IV, in the helical reduction in the static equilibrium MHD equations, the JFKO equation is separated and solutions are found again for two different types of pressure profiles. Both solutions have a radial dependence in terms of the confluent Heun function. Examples of the first type of pressure profile are shown, including one from Ref. 9 that arises as a special case. Examples of the second family of solutions

modeling stretched helically symmetric plasma configurations in a vacuum are also presented. In Sec. V, Galas–Bogoyavlenskij transformations are used to transform the solutions found in Secs. III and IV into non-stationary field-aligned physical exact solutions. The results are summarized and discussed in Sec. VI.

II. IDEAL PLASMA EQUILIBRIA WITH AXIAL AND HELICAL SYMMETRY
A. Magnetohydrodynamic systems

The isotropic MHD model (1.1) that describes ideal incompressible plasmas is an extension of Euler equations with a forcing term corresponding to the electrodynamic Lorentz force. For a quasi-neutral plasma with roughly an equal amount of ions and electrons, this force can be written as $\mathbf{f} = \mathbf{J} \times \mathbf{B}$. This isotropic model of plasma is suitable when the mean free path of plasma particles is much less than the typical length scale of the problem. Assumptions of infinite conductivity and negligible viscosity are valid for large magnetic and kinetic Reynolds numbers (cf. Ref. 2 and references therein).

In the dynamic equilibrium setting $\partial/\partial t = 0$, $\mathbf{V} \neq 0$, the MHD system (1.1) takes the following form:

$$\text{div}\,\rho\mathbf{V} = 0, \tag{2.1a}$$

$$\rho\mathbf{V} \times \text{curl}\,\mathbf{V} - \frac{1}{\mu}\mathbf{B} \times \text{curl}\,\mathbf{B} - \text{grad}\,P - \rho\,\text{grad}\frac{|\mathbf{V}|^2}{2} = 0, \tag{2.1b}$$

$$\text{curl}(\mathbf{V} \times \mathbf{B}) = 0, \tag{2.1c}$$

$$\text{div}\,\mathbf{B} = \text{div}\,\mathbf{V} = 0. \tag{2.1d}$$

From the incompressibility condition and the continuity equation, it follows that $\mathbf{V} \cdot \text{grad}\,\rho = 0$, which implies that in equilibrium flows the plasma density does not change along streamlines. The electric current density for an MHD plasma described by (1.1) or (2.1) is given by

$$\mathbf{J} = \frac{1}{\mu}\text{curl}\,\mathbf{B}. \tag{2.2}$$

A further reduction of (2.1) is the static equilibrium MHD system ($\mathbf{V} = 0$) given by

$$\text{div}\,\mathbf{B} = 0, \tag{2.3a}$$

$$\text{curl}\,\mathbf{B} \times \mathbf{B} = \mu\,\text{grad}\,P. \tag{2.3b}$$

In (2.3), a scaling transformation can be employed to pass to a dimensionless form with $\mu = 1$, which will be assumed below.

While multiple particular solutions of the above-mentioned plasma models (2.1) and (2.3) can be constructed, many fail to satisfy natural physical requirements. In addition to regularity and sufficient smoothness of the dependent variables $\mathbf{B}$, $\mathbf{V}$, P, and ρ, such requirements would include the requirement of finite kinetic and magnetic energies in the plasma domain $\mathcal{V}$,

$$\int_{\mathcal{V}} |\mathbf{V}|^2\,dV, \quad \int_{\mathcal{V}} |\mathbf{B}|^2\,dV < +\infty, \tag{2.4}$$

and the pressure asymptotics

$$P \to P_0 = \text{const as } |\mathbf{x}| \to +\infty. \tag{2.5}$$

Assuming non-negative pressure values, one requires $P_0 = 0$ for vacuum configurations, whereas $P_0 > 0$ corresponds to a plasma

supported by the pressure of an ambient medium. If the plasma domain is unbounded in one direction z, the finite energy requirement (2.4) may be restricted to a slice $z_1 \leq z \leq z_2$.

On the boundary surface $\partial \mathcal{V}$ of the plasma domain, the velocity is not generally required to vanish, but may satisfy the no-leak condition on $\partial \mathcal{V}$, which is given by takes the form $\mathbf{V} \cdot \mathbf{n} = 0$ in terms of the outside normal $\mathbf{n}$. The magnetic field also may be taken tangent to the boundary, $\mathbf{B} \cdot \mathbf{n} = 0$, on the "inside" side of $\partial \mathcal{V}$, and zero outside $\mathcal{V}$. In this case, the plasma domain boundary $\partial \mathcal{V}$ becomes a current sheet: indeed, the integration of the PDE (2.2) is a domain transverse to the boundary yields the surface electric current density given by

$$\mathbf{K} = \frac{\mathbf{B}}{\mu} \times \mathbf{n} \text{ on } \partial \mathcal{V}. \qquad (2.6)$$

An essential geometrical feature of dynamic MHD equilibria (2.1) is the existence of two-dimensional magnetic surfaces $\psi(\mathbf{x})$ = const that contain both the magnetic field lines and plasma streamlines: grad $\psi \cdot \mathbf{V} = $ grad $\psi \cdot \mathbf{B} = 0$ in $\mathcal{V}$. For bounded plasma domains, the domain boundary $\partial \mathcal{V}$, is a magnetic surface itself. For bounded $\mathcal{V}$, the magnetic surfaces are generally topologically equivalent to a set of nested tori,[31] and the magnetic field lines and plasma streamlines are dense on these surfaces. In the field-aligned case $\mathbf{V} = \lambda(\mathbf{x})\mathbf{B}$ as well as for Beltrami flows $\mathbf{V} = 0$, curl $\mathbf{B} = \alpha(\mathbf{x})\mathbf{B}$, magnetic surfaces may not be uniquely defined when magnetic field lines go to infinity or form closed curves.[32]

B. Axially symmetric equilibrium reduction

Both the dynamic and the static plasma equilibrium PDE systems (2.1) and (2.3) admit physical rotational and translational symmetries. In cylindrical coordinates (r, φ, z), the rotational symmetry is generated by the operator $X = \partial/\partial\varphi$, and rotationally invariant solutions of (2.3) have the following form:

$$\mathbf{B} = B^r(r,z)\mathbf{e}_r + B^\varphi(r,z)\mathbf{e}_\varphi + B^z(r,z)\mathbf{e}_z, \quad P = P(r,z). \qquad (2.7)$$

Bragg and Hawthorne,[25] and later Lüst and Schlüter,[33] Grad and Rubin,[26] and Shafranov[27] showed that in this case, the system (2.3) of four PDEs reduces to a single PDE (the Grad–Shafranov equation),

$$\psi_{rr} - \frac{1}{r}\psi_r + \psi_{zz} + I(\psi)I'(\psi) = -r^2 P'(\psi), \qquad (2.8)$$

satisfied by the stream function $\psi = \psi(r,z)$. The magnetic surfaces are defined by $\psi = $ const, and the magnetic field and the pressure are given by

$$\mathbf{B} = \frac{\psi_z}{r}\mathbf{e}_r + \frac{I(\psi)}{r}\mathbf{e}_\varphi - \frac{\psi_r}{r}\mathbf{e}_z, \quad P = P(\psi), \qquad (2.9)$$

where $I(\psi)$ and $P(\psi)$ are arbitrary functions constant on magnetic surfaces. [In (2.8) and (2.9), subscripts denote the respective partial derivatives, and primes denote the derivatives of I and P by their argument.] Various exact solutions of the Grad–Shafranov equation have been derived, in particular, when the terms $I(\psi)I'(\psi)$ and $P'(\psi)$ in (2.8) are linear in ψ. We especially note the explicit axially symmetric solutions obtained in Refs. 29 and 34 in spherical coordinates, corresponding, respectively, to a localized moving fluid vortex and a plasma ball, and Bogoyavlenskij's axially symmetric solutions modeling plasma jets,[8] given by a linear superposition

$$\psi(r,z) = e^{-\beta r^2}\left(a_N L_N^*(2\beta r^2) + \sum_{n=1}^{N-1} a_n \sin(\omega_n z + b_n) L_n^*(2\beta r^2)\right), \qquad (2.10)$$

in terms of the primitive functions L_n^* of the Laguerre polynomials, frequencies $\omega_n = \sqrt{8\beta(N-n)}$, arbitrary coefficients a_n, and phase shifts b_n, $n = 1, \ldots, N$. The solutions (2.10) arise for the linear Grad–Shafranov equation for the choice of arbitrary functions

$$I = \alpha\psi, \quad P = P_0 - 2\beta^2\psi^2, \qquad (2.11)$$

where P_0, α, and β are arbitrary constants. In Sec. III, we obtain a broader set of jet-like solutions of the plasma equilibrium model that includes (2.10) as a special case.

C. Helically symmetric equilibrium reduction

Helical coordinates (r, η, ξ) are defined in terms of cylindrical coordinates (r, φ, z) as

$$r, \quad \eta = \varphi + \gamma z/r^2, \quad \xi = z - \gamma\varphi, \qquad (2.12)$$

where γ is a constant parameter related to the helical pitch h by $h = 2\pi\gamma$ (Fig. 1). The helical coordinates reduce to polar coordinates when $\gamma = 0$. Unlike polar coordinates, for a general γ, the helical coordinates (r, η, ξ) are not orthogonal. However, one can introduce an orthogonal unit vector triple

$$\boldsymbol{e}_r = \frac{\nabla r}{|\nabla r|}, \quad \boldsymbol{e}_\xi = \frac{\nabla\xi}{|\nabla\xi|}, \quad \boldsymbol{e}_{\perp\eta} = \frac{\nabla_\perp\eta}{|\nabla_\perp\eta|} = \boldsymbol{e}_\xi \times \boldsymbol{e}_r, \qquad (2.13)$$

and express a generic vector field, for example, the magnetic induction $\mathbf{B}$ and the velocity $\mathbf{V}$, in that basis

$$\mathbf{B} = B^r\boldsymbol{e}_r + B^\varphi\boldsymbol{e}_\varphi + B^z\boldsymbol{e}_z = B^r\boldsymbol{e}_r + B^\eta\boldsymbol{e}_{\perp\eta} + B^\xi\boldsymbol{e}_\xi, \\ \mathbf{V} = V^r\boldsymbol{e}_r + V^\varphi\boldsymbol{e}_\varphi + V^z\boldsymbol{e}_z = V^r\boldsymbol{e}_r + V^\eta\boldsymbol{e}_{\perp\eta} + V^\xi\boldsymbol{e}_\xi. \qquad (2.14)$$
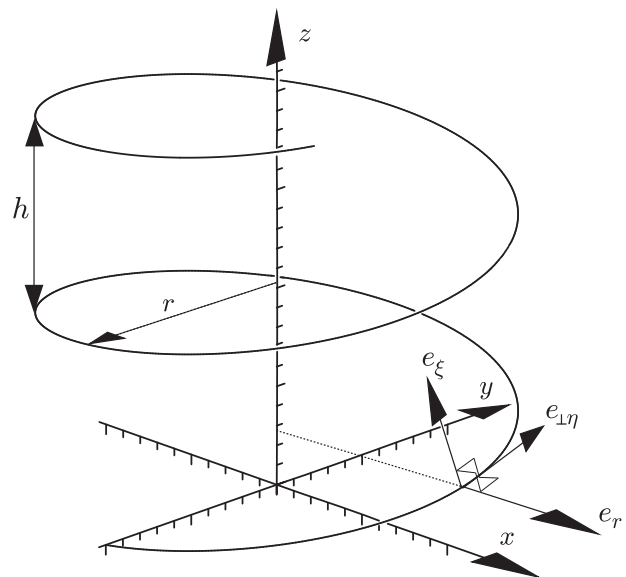

FIG. 1. Basis unit vectors in the helical coordinates. A helix $\xi = $ const for $\gamma = h/2\pi$, where h is the z-pitch of the helix.

The vector components in helical and cylindrical coordinates are related as follows:

$$B^{\eta} = \mathbf{B} \cdot \mathbf{e}_{\perp \eta} = Q\left(B^{\varphi} + \frac{\gamma}{r}B^z\right), \quad B^{\xi} = \mathbf{B} \cdot \mathbf{e}_{\xi} = Q\left(B^z - \frac{\gamma}{r}B^{\varphi}\right),$$

(2.15)

with the corresponding expressions for **V**. Here,

$$Q = Q(r) = \frac{r}{\sqrt{r^2 + \gamma^2}}.$$

(2.16)

Because the PDEs (2.1) and (2.3) admit rotational and translational symmetries generated by $\partial/\partial\varphi$ and $\partial/\partial z$, they also admit a symmetry generated by the linear combination $Y = \partial/\partial\varphi + \gamma \partial/\partial z$. The helical variables r and ξ are the invariants associated with the symmetry Y, and η is identified with a translational variable; see, e.g., Refs. 24 and 35. It turns out that imposing a helical symmetry $\partial/\partial\eta = 0$ on (2.3) is mathematically rather similar to the axial symmetry, and leads to a single PDE

$$\frac{\psi_{\xi\xi}}{r^2} + \frac{1}{r}\frac{\partial}{\partial r}\left(\frac{r}{r^2 + \gamma^2}\psi_r\right) + \frac{I(\psi)I'(\psi)}{r^2 + \gamma^2} + \frac{2\gamma I(\psi)}{(r^2 + \gamma^2)^2} = -\mu P'(\psi),$$

(2.17)

the famous Johnson–Frieman–Kulsrud–Oberman (JFKO) equation.[28] Similar to the axially symmetric case, the level surfaces of the flux function $\psi(r, \xi) = $ const define the magnetic surfaces, the pressure is constant on those surfaces, $P = P(\psi)$, and the magnetic field is given by

$$\mathbf{B} = \frac{\psi_{\xi}}{r}\mathbf{e}_r + \frac{rI(\psi) + \gamma\psi_r}{r^2 + \gamma^2}\mathbf{e}_{\varphi} + \frac{\gamma I(\psi) - r\psi_r}{r^2 + \gamma^2}\mathbf{e}_z.$$

(2.18)

Helically symmetric fluid and plasma flows admit additional structure, such as additional conservation laws.[23] Exact solutions of helically invariant flows include invariant solutions with respect to additional symmetry reductions and helically invariant Beltrami flows for the Navier–Stokes equations,[36] and jet-like solutions to (2.17) presented in Ref. 9. The latter are separated solutions that arise for the choice of arbitrary functions (2.11) that make the JFKO equation (2.17) linear

$$\psi_{Nmn}(r, \xi) = e^{-\beta r^2}\left(a_N B_{0N}(s) + r^m B_{mn}(s)\right.$$
$$\left. \times \left(a_{mn}\cos\frac{m\xi}{\gamma} + b_{mn}\sin\frac{m\xi}{\gamma}\right)\right),$$

(2.19)

where N, m, and n are arbitrary positive integers, $s = 2\beta r^2$ is a rescaled radial variable, and the functions $B_{mn}(s)$ are polynomials of degree n related to the Laguerre polynomials. Superpositions of the separated solutions $\psi_{Nmn}(r, \xi)$ yield new solutions of the JFKO equation with multiple arbitrary parameters.[9] In Sec. IV, we obtain a broader set of jet-like solutions of the plasma equilibrium model that includes separated solutions (2.19) and their combinations as special cases.

III. NEW EXACT AXIALLY SYMMETRIC PLASMA EQUILIBRIA

The Grad–Shafranov equation (2.8) becomes linear when the arbitrary functions have the following form (2.11):

$$P(\psi) = P_0 + b\psi + \frac{1}{2}a\psi^2, \quad I(\psi) = \alpha\psi,$$

(3.1)

where $a, b, \alpha = $ const. The linear homogeneous case corresponds to $b = 0$ and includes (2.11) when $a < 0$. For (3.1) with $b = 0$, the Grad–Shafranov equation is given by

$$\psi_{rr} - \frac{1}{r}\psi_r + \psi_{zz} + (\alpha^2 + ar^2)\psi = 0,$$

(3.2)

and admits separated solutions $\psi(r, z) = R(r)Z(z)$ satisfying

$$Z'' = \lambda Z, \quad R'' - \frac{1}{r}R' + (\alpha^2 + ar^2 + \lambda)R = 0,$$

(3.3)

where λ is an arbitrary separation constant. Depending on the value of a in the pressure term, one obtains two families of solutions corresponding to two different types of pressure profiles. For the family with $a < 0$, assuming plasma pressure is non-negative-definite, $P \rightarrow P_0 > 0$ when $|\mathbf{x}| \rightarrow \infty$, and pressure values $P < P_0$ occur within the plasma domain $\mathcal{V}$. For the second family with $a > 0$, one may choose $P > 0$ inside $\mathcal{V}$ and $P = 0$ outside. The latter corresponds to physical applications such as laboratory plasma confinement devices and astrophysical plasma jets propagating in a vacuum (cf. Sec. II A).

A. The first family of axially symmetric solutions

The first family of solutions arises when $a = -q^2 < 0$. This corresponds to the pressure profile $P(\psi) = P_0 - \frac{1}{2}q^2\psi^2$ bounded above by P_0, and, thus, models axially symmetric plasma configurations in an ambient medium. When the separation constant is a negative value $\lambda = -k^2$, $k > 0$, the corresponding separated solution describes a plasma extended along the z axis. From (3.3), one has

$$Z = C_3 \sin(kz) + C_4 \cos(kz).$$

(3.4)

To solve the radial differential equation from (3.3), the substitution $s = qr^2$, $R(r) = S(s)$ can be used to transform this equation into the following form:

$$S'' + \left(-\frac{1}{4} + \frac{\alpha^2 - k^2}{4qs}\right)S = 0,$$

(3.5)

which is related to the Whittaker ODE (ordinary differential equation)

$$y''(s) + \left(-\frac{1}{4} + \frac{\delta}{s} + \frac{1/4 - \nu^2}{s^2}\right)y(s) = 0,$$

(3.6)

when

$$\delta = \frac{\alpha^2 - k^2}{4q}, \quad \nu = \frac{1}{2}.$$

(3.7)

From the general solution $y(s) = C_1 W_M(\delta, \nu, s) + C_2 W_W(\delta, \nu, s)$ of the Whittaker ODE in terms of the two Whittaker basis functions, one, thus, obtains the general solution to (3.5). The corresponding separated solution of the linear Grad–Shafranov equation (3.2) is consequently given by

$$\psi_k(r, z) = \left(C_1 W_M\left(\delta, \frac{1}{2}, qr^2\right) + C_2 W_W\left(\delta, \frac{1}{2}, qr^2\right)\right)$$
$$\times (C_3 \sin kz + C_4 \cos kz),$$

(3.8)

where C_1, C_2, C_3, and C_4 are free constants. It should be noted that due to the linearity of (3.2), any linear combination of functions (3.8) yield solutions to (3.2), including

$$\Psi(r,z) = \int_{-\infty}^{\infty} \psi_k(r,z)\, dk, \qquad (3.9)$$

where $C_i = C_i(k)$, $i = 1, 2, 3, 4$, are arbitrary suitable distributions. It should be noted that with the choice of C_i,

$$C_1(k) = \sum_{n=1}^{N-1} \tilde{a}_n \Delta\left(k - \sqrt{\alpha^2 - 4qn}\right), \quad C_2(k) = 0,$$
$$C_3 = a_n \cos b_n, \quad C_4 = a_n \sin b_n, \qquad (3.10)$$

where $\Delta(\mathbf{x})$ denotes the Dirac delta function, (3.9) yields Bogoyavlenskij's solution (2.10). This corresponds to (3.8) having $\delta \in \mathbb{N}$.

It is easy to show that the separated solution (3.8) is globally regular only when $\delta \in \mathbb{N}$ (see Appendix A). The global regularity, in the sense of the absence of singularities of the magnetic field components on the axis and sufficiently fast decay away from it, is, thus, the feature of Bogoyavlenskij's solutions (2.10). However, as shown below, the solutions (3.8) for general δ can be used to describe physical plasmas in domains bounded in the radial direction.

1. The first family of axially symmetric solutions: Example 1

Two examples are considered for the first solution family. The first utilizes the separated solution (3.8) for a case when δ is not a positive integer. It should be noted that to achieve finite magnetic energy, the domain of this solution needs to be restricted, with the physical boundary involving a current sheet such as in formula (2.6). The magnetic surfaces and pressure values for the first example are shown in Fig. 2(a), the magnetic energy density is shown in Fig. 2(b), and the absolute value of the current density in Fig. 2(c), for the solution parameters indicated therein. The dotted line marks the boundary of the plasma domain.
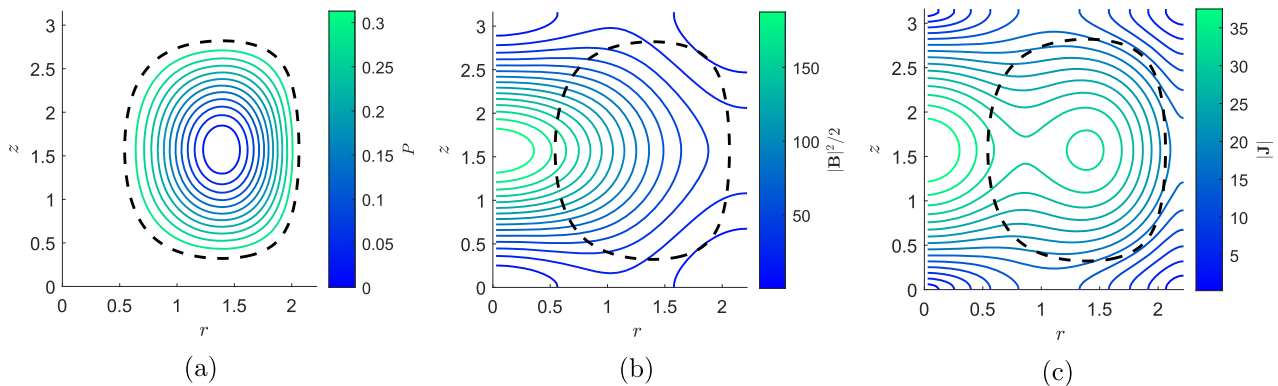
2. The first family of axially symmetric solutions: Example 2

The second example of first family of axial solutions is a linear combination of the special case of (3.8) when δ given by (3.7) takes on positive integer values; this yields Whittaker functions related to the Laguerre polynomials. This type of solutions was discussed in Ref. 8 [see formula (2.10)]. A sample cross section of the magnetic surfaces and pressure values is shown in Fig. 3(a), and contour plots of magnetic energy density and current density in Figs. 3(b) and 3(c). In this example, the magnetic field and currents are concentrated about the center of the plasma jet, with $|\mathbf{B}|, |\mathbf{J}| \to 0$ as $r \to \infty$. Far from the axis, the pressure satisfies $P \to P_0 = \text{const}$; therefore, this global solution corresponds to a plasma propagating in the ambient medium.

B. The second family of axially symmetric solutions

The next family of new solutions arises when $a = q^2 > 0$. This corresponds to plasmas residing in vacuum: $P = 0$ outside of the plasma domain $\mathcal{V}$, and with $P > 0$ inside $\mathcal{V}$. The separated solution part for $Z(z)$ given by (3.4) can be used. After transforming the radial problem from (3.3) with $x = iqr^2$, where i is the imaginary unit, the following ODE related to the Whittaker equation ODE (3.6) is obtained (Fig. 3):

$$R'' + \left(-\frac{1}{4} + i\frac{k^2 - \alpha^2}{4qx}\right)R = 0. \qquad (3.11)$$

Its general solution can be written in terms of Whittaker functions of a complex argument and a complex parameter

$$R(r) = C_1 W_M\left(-i\delta, \frac{1}{2}, iqr^2\right) + C_2 W_W\left(-i\delta, \frac{1}{2}, iqr^2\right), \qquad (3.12)$$

where δ is given by (3.7).

The solution (3.12) can be written in terms of real-valued functions and free constants, using a relationship between the Whittaker functions and the Coulomb wave functions
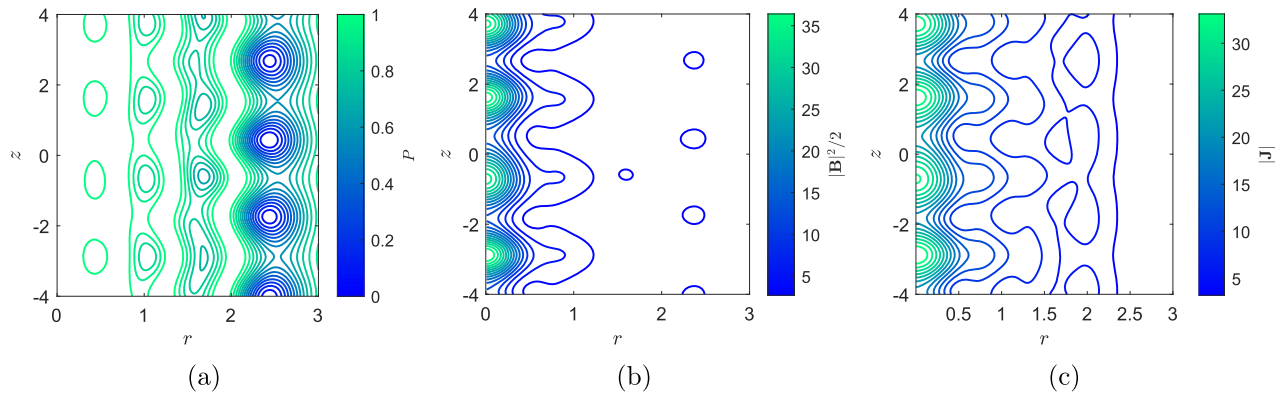

(a)　　　　　　　　　　　(b)　　　　　　　　　　　(c)

FIG. 2. (a) A cross section of magnetic surfaces $P = \text{const}$ for an axially symmetric plasma equilibrium solution belonging to Family 1 (3.8), with $C_1 = 10^2$, $C_2 = 0$, $C_3 = 1$, $C_4 = 0$, $q = 0.1$, $\alpha = 2$, and $k = 1$. The bounding surface of the plasma domain is given by $P_0 = 3.48 \times 10^{-5}$ and is shown with the dashed line. The dimensionless pressure $P = P_0 - q^2\psi^2/2$ satisfies $P > 0$ inside this domain. (b) and (c) The corresponding magnetic energy density $|\mathbf{B}|^2/2$ and the magnitude of the current density $|\mathbf{J}|$.

FIG. 3. A cross section of axially symmetric magnetic surfaces $P = \text{const}$ (first solution family with $\delta \in \mathbb{N}$). (a) The colorbar shows the values of the dimensionless pressure $P = P_0 - q^2\psi^2/2$, (b) the magnetic energy density $|\mathbf{B}|^2/2$, and (c) the magnitude of the current density $|\mathbf{J}|$.

$$W_M\left(-i\delta, \frac{1}{2}, iqr^2\right) = 2\,i\,\frac{\mathcal{C}_F(0, -\delta, qr^2/2)}{|\Gamma(1 - i\delta)|}e^{\delta - \pi/2}. \quad (3.13)$$

This provides the motivation to transform the radial problem (3.3) into a related one of the Coulomb ODE type using $x = qr^2/2$, which yields

$$R'' + \left(1 + 2\frac{\alpha^2 - k^2}{4qx}\right)R = 0, \quad (3.14)$$

and is related to the Coulomb wave ODE

$$y''(s) + \left(1 - \frac{2\sigma}{s} - \frac{L(L+1)}{s^2}\right)y(s) = 0, \quad (3.15)$$

with constant parameters σ and L. The Coulomb equation has the general solution $y(s) = C_1\,\mathcal{C}_F(L, \sigma, s) + C_2\,\mathcal{C}_G(L, \sigma, s)$ in terms of the two basis Coulomb special functions. One, thus, arrives at

$$R(r) = C_1\,\mathcal{C}_F\left(0, -\delta, \frac{q}{2}r^2\right) + C_2\,\mathcal{C}_G\left(0, -\delta, \frac{q}{2}r^2\right). \quad (3.16)$$

The second family of solutions to (3.2) corresponding to plasma confined in a vacuum is, therefore, given by

$$\psi_k(r, z) = \left(C_1\,\mathcal{C}_F\left(0, -\delta, \frac{q}{2}r^2\right) + C_2\,\mathcal{C}_G\left(0, -\delta, \frac{q}{2}r^2\right)\right)$$
$$\times (C_3 \sin kz + C_4 \cos kz), \quad (3.17)$$

where δ (3.7) is the same as the first family. Again, any linear combination of the above-mentioned separated solution is also a solution

$$\Psi(r, z) = \int_{-\infty}^{\infty} \psi_k(r, z)\,dk, \quad (3.18)$$

where $C_i = C_i(k)$, $i = 1, 2, 3, 4$ are integrable functions or distributions. It should be noted that due to the nature of $\mathcal{C}_F$ and $\mathcal{C}_G$, (3.17) may not globally not satisfy requirements stated in Sec. II but may have finite magnetic energy and positive internal pressure in a subdomain of $\mathbb{R}^3$ surrounded by a current sheet [formula (2.6)].

1. The second family of axially symmetric solutions: Examples

Solution belonging to the second family may be z-periodic, such as separated solutions (3.17) for single k values or linear combinations of solutions with rational k value ratios (Fig. 4) or non-periodic otherwise. An example of a quasiperiodic solution is shown in Fig. 5. In that example, the solution is given by a linear combination

$$\psi_k(r, z) = \psi_{k_1}(r, z) + 0.75\psi_{k_2}(r, z), \quad (3.19)$$

where $k_1 = 2$, $k_2 = \sqrt{2}$, the values $\alpha = 5$ and $q = \sqrt{3}$ defining $P(\psi)$ and $I(\psi)$ are common for ψ_{k_1} and ψ_{k_2}, and the respective sets of constant C_1, C_2, C_3, C_4 are given by $(1, 0, 1, 1)$ and $(1, 0, 1, 0)$.

For the solutions of this family, magnetic surfaces given by nested tori, and the locally highest pressure values are on the toroidal axes. A spatially bounded plasma equilibria can be obtained through the truncation of a solution to some toroidal magnetic surface that defines the boundary of the plasma domain, and the introduction of a current sheet. On the bounding magnetic surface, one may choose $P = 0$, and consequently have $P > 0$ in the plasma domain, which corresponds to a plasma equilibrium in a vacuum.

IV. HELICALLY SYMMETRIC EXACT PLASMA EQUILIBRIA AND EXACT SOLUTIONS

Similarly to the axially symmetric case, helically symmetric plasma configurations are described by a *linear* JFKO equation (2.17),

$$\frac{1}{r^2}\frac{\partial^2\psi}{\partial\xi^2} + \frac{1}{r}\frac{\partial}{\partial r}\left(\frac{r}{r^2 + \gamma^2}\frac{\partial\psi}{\partial r}\right) + \frac{\alpha^2\psi}{r^2 + \gamma^2} + \frac{2\gamma\alpha\psi}{(r^2 + \gamma^2)^2} + \sigma\psi = -b, \quad (4.1)$$

when the pressure P is a quadratic and I a linear function of ψ,

$$P(\psi) = P_0 + b\psi + \frac{1}{2}\sigma\psi^2, \quad I(\psi) = \alpha\psi. \quad (4.2)$$

The second order PDE is linear homogeneous when $b = 0$. It admits separated solutions $\psi(r, u) = R(r)\Xi(\xi)$ satisfying
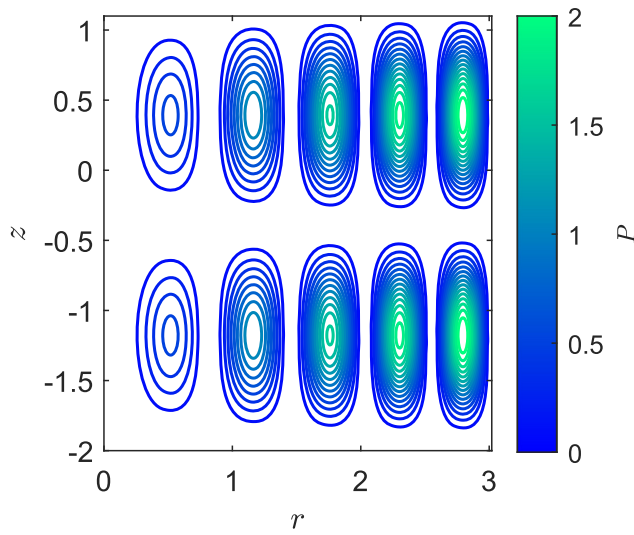
$$\Xi'' = \lambda\Xi, \quad (4.3a)$$

FIG. 4. A cross section of magnetic surfaces $\psi, P = \text{const}$ for a sample axially symmetric z-periodic plasma equilibrium solution belonging to a Family 2, (3.17), with $C_1 = 1$, $C_2 = 0$, $C_3 = 1$, $C_4 = 1$, $k = 2$, $\alpha = 5$, and $q = \sqrt{3}$. The configuration is z-periodic. The colorbar shows the values of the dimensionless pressure $P = P_0 + q^2\psi^2/2$.

$$r\left(\frac{r}{r^2 + \gamma^2}R'\right)' + \left(\frac{\alpha^2 r^2}{r^2 + \gamma^2} + \frac{2\gamma\alpha r^2}{(r^2 + \gamma^2)^2} + \sigma r^2\right)R = -\lambda R. \quad (4.3b)$$

Here, the separation constant, λ is taken negative: $\lambda = -\omega^2$, which, as with the axial case, corresponds to a model of a plasma jet stretched along the z axis: the helical part Ξ is given by

$$\Xi(\xi) = C_1 \sin(\omega\xi) + C_2 \cos(\omega\xi). \quad (4.4)$$

in terms of arbitrary C_1 and C_2. Depending on the value of σ in the pressure term of (4.2), one again obtains two different families of solutions $R(r)$. Similarly to the axial cases discussed above, these solutions correspond to two different types of pressure profiles. For $\sigma < 0$, $P \leq P_1 = \text{const} > 0$, with $P \to P_1$ when $|\mathbf{x}| \to \infty$. For the other case when $\sigma > 0$, one can choose $P > 0$ inside of the plasma domain $\mathcal{V}$ and $P = 0$ outside of $\mathcal{V}$.

A. The first family of helically symmetric solutions

The first family of solutions arises when $\sigma = -\kappa^2 < 0$, that is, the pressure is given by $P(\psi) = P_0 - (\kappa^2\psi^2)/2$, being bounded from above by some P_0, with $P \to P_0$ when $|\mathbf{x}| \to \infty$, and models plasmas supported by in a surrounding medium. Upon the substitution of this pressure form and $\lambda = -\omega^2$ the following equation on $R(r)$ arises:
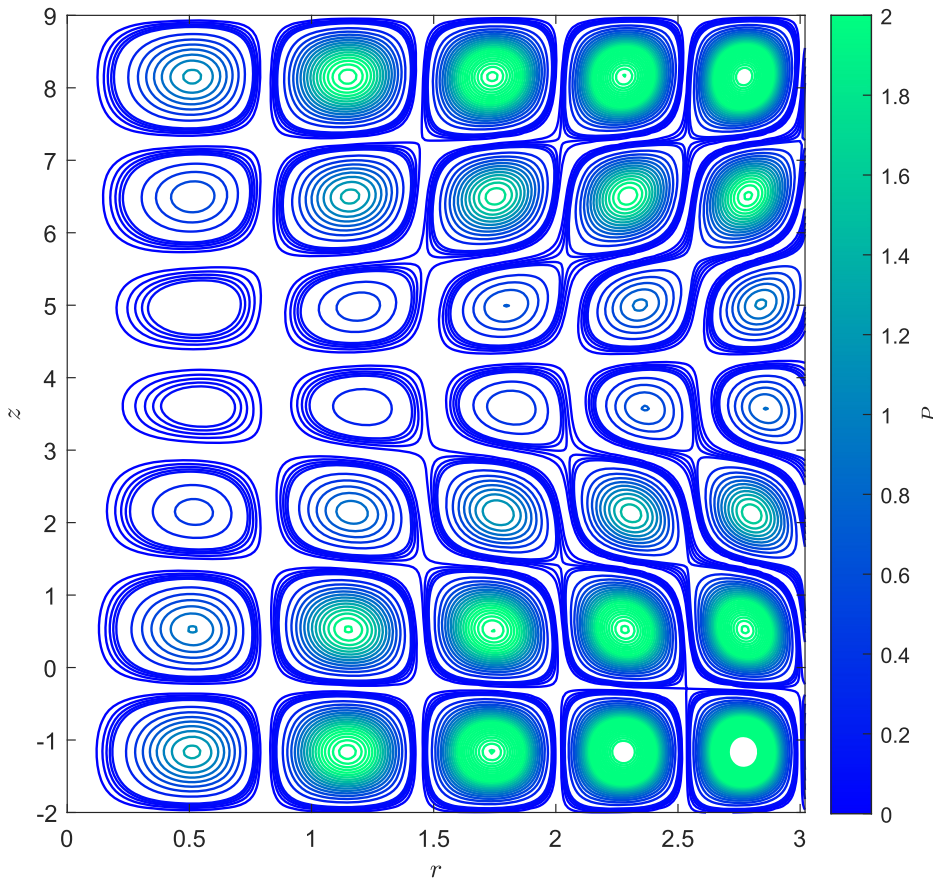

FIG. 5. A cross section of axially symmetric magnetic surfaces $\psi, P = \text{const}$ for a non-z-periodic solution (3.19).

$$r\left(\frac{r}{r^2+\gamma^2}R'\right)' + \left(\frac{\alpha^2 r^2}{r^2+\gamma^2} + \frac{2\gamma\alpha r^2}{(r^2+\gamma^2)^2} - \kappa^2 r^2\right)R = \omega^2 R. \quad (4.5)$$

The solution can be written, for example, in terms of a pair of confluent Heun functions

$$R(r) = e^{-\kappa r^2/2}\left(C_1 r^b \mathcal{H}_C(a, b, -2, c, d, -r^2/\gamma^2)\right.$$
$$\left. + C_2 r^{-b}\mathcal{H}_C(a, -b, -2, c, d, -r^2/\gamma^2)\right), \quad (4.6a)$$

where

$$a = \kappa\gamma^2, \quad b = \gamma\omega, \quad c = \frac{\gamma^2(\gamma^2\kappa^2 - \alpha^2 + \omega^2)}{4}, \quad (4.6b)$$

and

$$d = 1 - \frac{\kappa^2\gamma^4}{4} + \frac{\alpha^2 - \omega^2}{4}\gamma^2 + \frac{\alpha\gamma}{2}. \quad (4.6c)$$

The above Heun functions form a basis of solutions of the confluent Heun equation

$$y'' - \frac{(-x^2 a + (-b+a)x + b + 1)}{x(x-1)}y'$$
$$- \frac{((-ba - 2c)x + (b+1)a + b - 2d + 2)}{2x(x-1)}y = 0, \quad (4.7)$$

that involves the parameters a, b, c, and d.

There exists necessary and sufficient conditions for the confluent Heun function to yield polynomials, which are discussed thoroughly in Ref. 37. These solutions correspond to solutions constructed in Ref. 9. In particular, for the confluent Heun function $\mathcal{H}_C(\alpha, \beta, -2, \delta, \eta, x)$, a necessary condition for the emergence of these polynomials is $\delta = -\alpha(n + \beta/2)$, where n is a positive integer that specifies the degree of this polynomial. The sufficient condition comes from choosing characteristic values of η that correspond to roots of the coefficient of the $(n + 1)$ degree of the series expansion. Further details can be found in Ref. 37.

To explicitly avoid singularities at the origin, in examples that follow, C_2 will be set to zero. In this case, the separated solution family can be written as

$$\psi_\omega(r, \xi) = e^{-\kappa r^2/2}r^b \mathcal{H}_C(a, b, -2, c, d, -r^2/\gamma^2)(C_1 \sin(\omega\xi)$$
$$+ C_2 \cos(\omega\xi)). \quad (4.8)$$

A general class of solutions can be constructed as a discrete or continuous linear combination of (4.8)

$$\psi(r, \xi) = \int_{-\infty}^{\infty} \psi_\omega(r, \xi)\,d\omega, \quad C_i = C_i(\omega), \quad i = 1, 2. \quad (4.9)$$

1. Examples of the first family of helically invariant solutions

Separated solutions (4.8) given in terms of the confluent Heun function contain a special case when the Heun function reduces to a polynomial [see formula (2.19)]; this case was discussed in detail in Ref. 9.

The first example illustrates the general case when Heun functions are not given by polynomials. The (x, y)-plane cross section of the separated solution (4.8) with parameters

$$\alpha = 5.9, \quad \kappa = 1, \quad \gamma = 1, \quad \omega = 3/\gamma, \quad (4.10)$$

is shown in Fig. 6. The helical magnetic surfaces are helical cylinders obtained by simultaneous lifting (along z) and rotation (around z) of the shape in Fig. 6(a). The dashed line denotes a possible boundary magnetic surface of the plasma configuration. The ambient pressure value P_0 is chosen so that $P = 0$ on the magnetic axis of each helical cylinder.

The second example where linear combination of separated solutions (4.8),

$$\psi = \psi_1 - \frac{\pi}{4}\psi_2, \quad (4.11)$$

where ψ_1 is defined by the parameters (4.10), and for ψ_2, $\omega = \sqrt{3}/\gamma$, yields non-z-periodic magnetic surfaces shown in Fig. 7.

The third example from the first family of helically invariant solutions is for the special case when the separated solution simplifies to a product of a decaying exponential and polynomials [formula (2.19)]. This subfamily of global solutions was obtained by Bogoyavlenskij.[9] Magnetic surfaces, pressure contours, and the corresponding magnetic energy density are shown in Fig. 8.
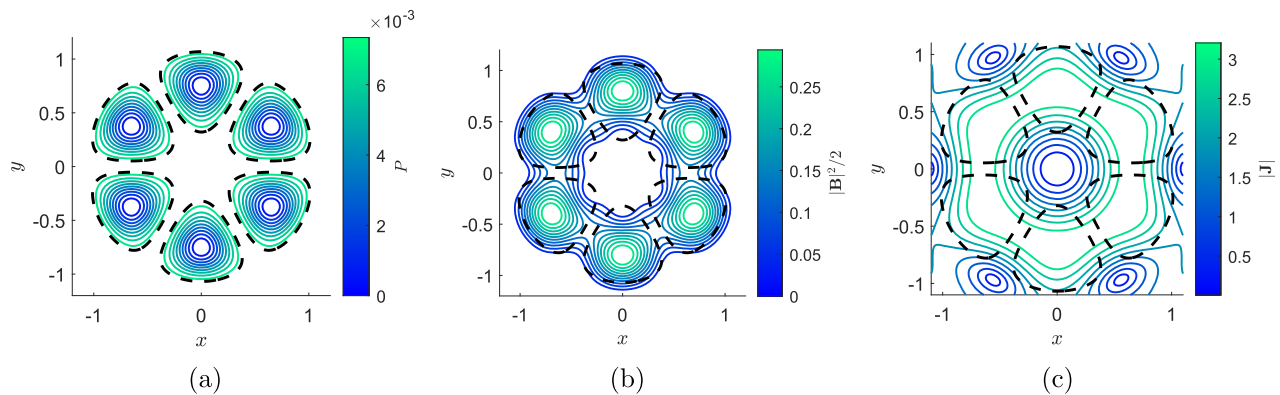
FIG. 6. The (x, y)-cross section of a truncated helically symmetric physical solution from the first family. The pressure contour, magnetic energy density, and current density magnitude can be seen from left to right.
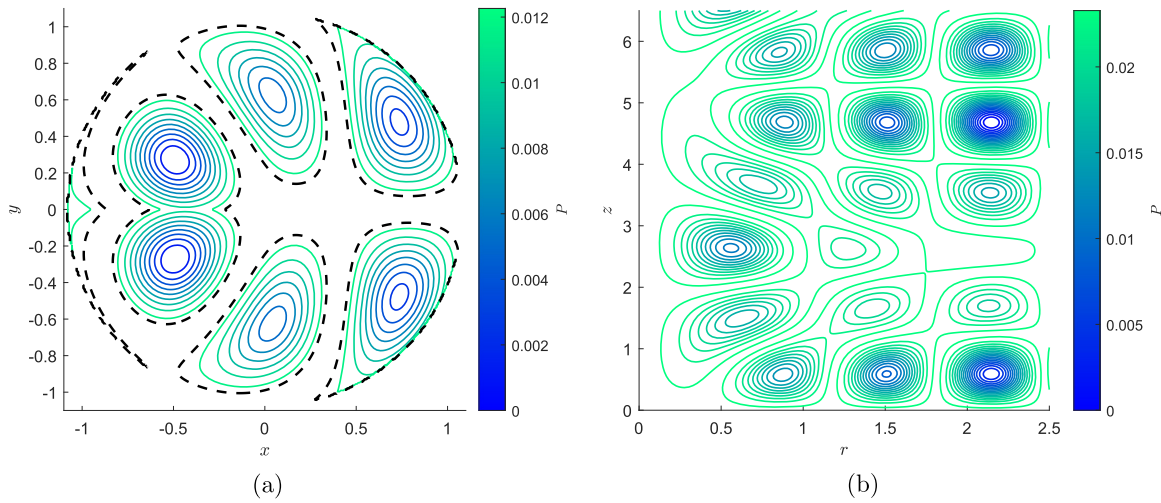
FIG. 7. Magnetic surfaces and pressure values for a linear combination (4.11) of helically invariant separated solutions (4.8) from the first helically invariant family, corresponding to the same forms of $P(\psi)$ and $I(\psi)$ in the JFKO model (4.1). (a) An (x, y)-plane cross section and (b) An (r, z)-plane cross section.

B. The second family of helically symmetric solutions

The second family arises when in (4.1) and (4.2), $\sigma = \kappa^2 > 0$. This corresponds to the case when the pressure is higher inside the plasma domain and lower outside, and is suitable to describe plasmas in vacuum. The radial component satisfies the ODE (4.3b) with $\sigma = \kappa^2$; its solution can be expressed in terms of the confluent Heun functions with a complex exponential and complex parameters

$$R(r) = e^{-i\kappa r^2/2}\big(C_1 r^b \mathcal{H}_C(ia, b, -2, c, d, -r^2/\gamma^2) + C_2 r^{-b} \mathcal{H}_C(ia, -b, -2, c, d, -r^2/\gamma^2)\big), \quad (4.12)$$

where a, b, c, and d are given above in (4.6). As above, we set $C_2 = 0$ in (4.12). It is not obvious but is true that (4.12) yields a real-valued function. Keeping the regular part of (4.12), we consequently find that a

separated solution to (4.1) corresponding to helically symmetric plasma in a vacuum or a lower pressure environment is generally given by

$$\psi_\omega(r, \xi) = e^{-i\kappa r^2/2} r^b \mathcal{H}_C(ia, b, -2, c, d, -r^2/\gamma^2) \\ \times (C_1 \sin(\omega\xi) + C_2 \cos(\omega\xi)). \quad (4.13)$$

A solution family is obtained as a discrete or a continuous linear combination of (4.13)

$$\psi(r, \xi) = \int_{-\infty}^{\infty} \psi_\omega(r, \xi)\, d\omega, \quad (4.14)$$

where $C_1 = C_1(\omega)$, $C_2 = C_2(\omega)$ are arbitrary weighting distributions.

Similarity to the Coulomb wave functions for axially symmetric equilibria (Sec. III B), the radial part $R(r)$ (4.12) is a quasiperiodic
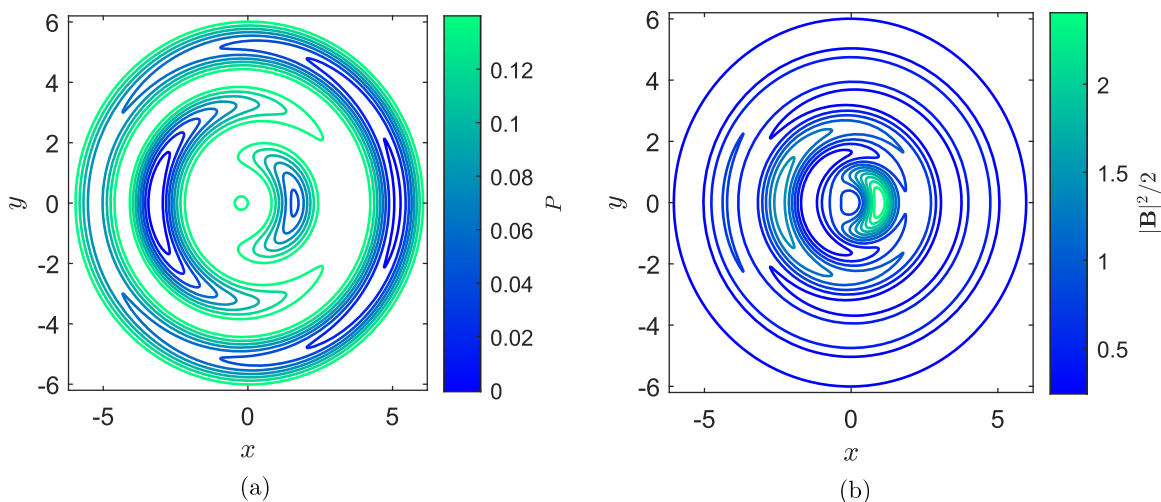

FIG. 8. (a) Helically symmetric magnetic surfaces and pressure values $P = $ const for the first family of solutions: a sample exponential-polynomial solution $\Psi(r, \xi)$ (2.19) with $N = 4$, $n = 0$, $m = 1$, $\kappa = 0.2$, $\gamma = 1$, $a_N = a_n = 1$, and $b_n = 0$. (b) The corresponding magnetic energy density values.
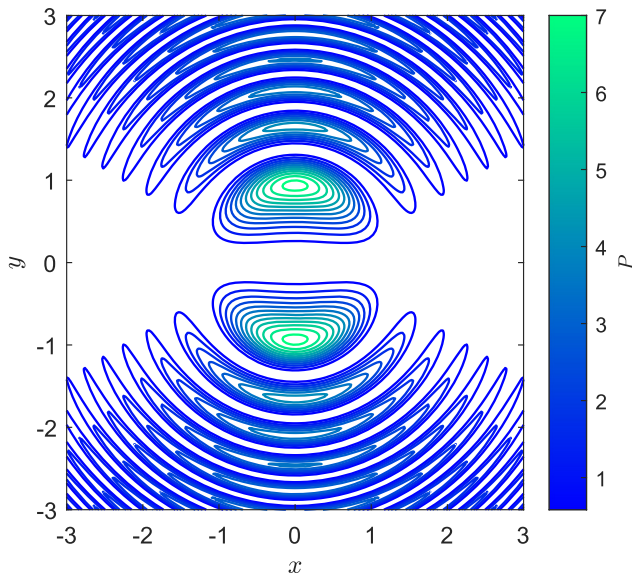
06 February 2024 19:55:52

FIG. 9. A cross section of magnetic surfaces ψ, $P = $ const for a sample separated helically symmetric plasma equilibrium solution belonging to the second family (4.13) with parameter choices (4.15). The colorbar shows the values of the dimensionless pressure $P = \kappa^2 \psi^2 / 2$.

function, and consequently, for a physical plasma equilibrium, plasma domain must be restricted to within some chosen magnetic surface $\psi = \psi_0$ outside of which P and $\mathbf{B} = 0$. This is again accomplished by utilizing the boundary condition (2.6).

1. An example of the second family of helically invariant solutions

We now illustrate separated solutions (4.12), choosing the helical pitch parameter γ and the arbitrary constants as follows:
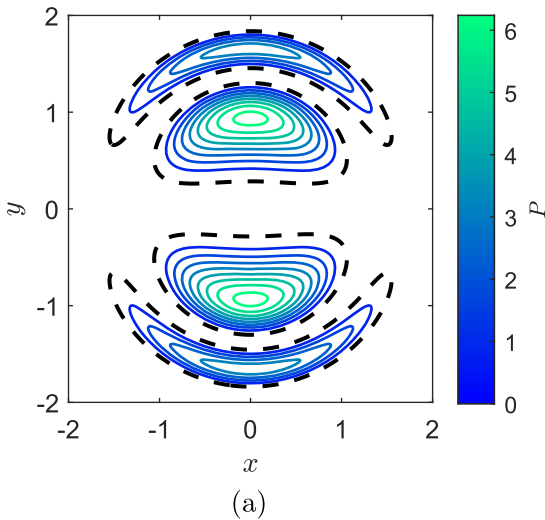
$$\gamma = 1, \quad C_1 = 1, \quad C_2 = 0, \quad \alpha = 3, \quad \kappa = 4, \quad \omega = 1, \quad P_0 = 0. \tag{4.15}$$

The global contours of the pressure $P(\psi) = \kappa^2 \psi^2 / 2$ are shown in Fig. 9. We note the radial periodic behavior similar to the Coulomb wave functions in the axially symmetric case (Fig. 4). It appears that for the type of pressure configuration suitable for a plasma residing in vacuum the solutions for both axial symmetry and helical symmetry have oscillatory nature in the radial variable. Details for the same configuration truncated at a certain magnetic surface is shown in Fig. 10.

V. GENERALIZATIONS TO DYNAMIC EQUILIBRIA

Galas[38] and Bogoyavlenskij[39] established a family of nonlocal symmetries of the dynamic MHD equilibrium equations (2.1) (see also Ref. 40). If $\mathbf{V}$, $\mathbf{B}$, P, and ρ is a solution of (2.1), where the density ρ is constant on both magnetic surfaces (or more generally, on magnetic field lines and plasma streamlines), then there exists an infinite family of solutions $\mathbf{V}_1$, $\mathbf{B}_1$, P_1, and ρ_1 which, for a general μ, can be constructed by

$$\mathbf{B}_1 = b(\psi)\mathbf{B} + c(\psi)\sqrt{\mu\rho}\mathbf{V}, \quad \mathbf{V}_1 = \frac{c(\psi)}{a(\psi)\sqrt{\mu\rho}}\mathbf{B} + \frac{b(\psi)}{a(\psi)}\mathbf{V},$$
$$P_1 = CP + \frac{C\mathbf{B}^2 - \mathbf{B}_1^2}{2\mu}, \quad \rho_1 = a^2(\psi)\rho. \tag{5.1}$$

In (5.1), $a(\psi)$ and $b(\psi)$ are arbitrary functions constant on both magnetic fields lines and streamlines, and $b^2(\psi) - c^2(\psi) = C = $ const is a free constant. The transformation (5.1) preserves the magnetic surfaces of the initial plasma configuration ($\mathbf{V}$, $\mathbf{B}$, P, ρ). In particular, starting from a static equilibrium with $\mathbf{V} = 0$, the transformations (5.1) produce an infinite set of solutions of the MHD system (2.1) with motion: $\mathbf{V} \neq 0$. Choosing, for example,

$$F_1(\psi) = c(\psi), \quad F_2(\psi) = a(\psi)\sqrt{\rho}, \tag{5.2}$$

as free functions, one can map a static equilibrium ($\mathbf{B}$, P) to a dynamic equilibrium solution family
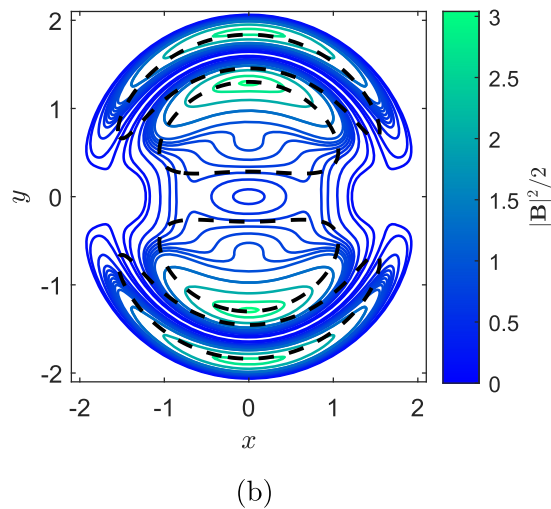

(a)

(b)

FIG. 10. Truncated magnetic surfaces $P = $ const for the helically symmetric plasma equilibrium solution belonging to the second family (4.13) with parameter choices (4.15) and boundary condition (2.6). (a) Magnetic surfaces and pressure values and (b) the corresponding magnetic energy density values.

$$\mathbf{B}_1 = \sqrt{C + F_2^2(\psi)}\, \mathbf{B}, \quad \mathbf{V}_1 = \frac{F_1^2(\psi)}{F_2^2(\psi)\sqrt{\mu}}\, \mathbf{B},$$

$$P_1 = CP - F_1^2(\psi)\frac{\mathbf{B}^2}{2\mu}, \quad \rho_1 = F_2^2(\psi), \tag{5.3}$$

and, thus, transform the new axially and helically symmetric static exact solutions constructed in Secs. III and IV into further new dynamic solutions with $\mathbf{V}_1 \neq 0$. All such dynamic solutions are field-aligned: $\mathbf{V}_1 \parallel \mathbf{B}_1$.

Note that the pressure in the dynamic MHD equilibrium model (2.1) in general, and the transformed pressure P_1 in (5.3), in particular, are generally *not constant* on magnetic surfaces. It is also useful to note that Galas–Bogoyavlenskij transformations preserve the difference of kinetic and magnetic energy densities[32]

$$\frac{\rho_1 |\mathbf{V}_1|^2}{2} - \frac{|\mathbf{B}_1|^2}{2\mu} = \frac{\rho |\mathbf{V}|^2}{2} - \frac{|\mathbf{B}|^2}{2\mu}. \tag{5.4}$$

A. Example: A dynamic transformation of a new axially symmetric solution

For the example of Sec. III A 1 (Fig. 2), denote the static magnetic field by $\mathbf{B}_{st}$. The pressure is given by $P = P_0 - (q^2\psi^2)/2$, and the magnetic flux ψ by (3.8). Choosing the dimensionless free functions (5.2) to be

$$F_1(\psi) = \frac{0.075}{1+\psi}, \quad F_2(\psi) = 1 + 0.7(P(\psi))^{1/2}, \tag{5.5}$$

and letting $C = 1$, one transforms the static axially symmetric plasma equilibrium $(\mathbf{B}_{st}, P)$ into a dynamic axially symmetric equilibrium $(\mathbf{V}_1, \mathbf{B}_1, P_1, \rho_1)$ (5.3). The pressure profiles and magnetic and kinetic energy densities for the new dynamic solution is shown in Fig. 11.

B. Example: A new dynamic helically symmetric plasma equilibrium configuration

Taking as a starting solution the second family of static helically symmetric solutions of shown in Sec. IV B 1, with the magnetic field components and pressure given by

$$\mathbf{B}_{st} = \frac{\psi_\xi}{r}\mathbf{e}_r + \frac{\alpha r\psi + r\psi_r}{r^2 + \gamma^2}\mathbf{e}_\varphi + \frac{\gamma\alpha\psi - r\psi_r}{r^2 + \gamma^2}\mathbf{e}_z, \quad P = P_0 + \frac{\kappa^2}{2}\psi^2, \tag{5.6}$$

where ψ is given by (4.13) and (4.15), and using the two arbitrary functions forms

$$F_1(\psi) = 2\psi^2, \quad F_2(\psi) = 1 + \psi, \tag{5.7}$$

and $C = 1$, through the transformation (5.3), we obtain a new dynamic solution $(\mathbf{V}_1, \mathbf{B}_1, P_1, \rho_1)$, $\mathbf{V}_1 \neq 0$. The cross-sectional contours of the magnetic surfaces of the static configuration (4.13) and (4.15), the original profile of the pressure P, the contours of the transformed pressure P_1, and the magnetic energy density are plotted in Figs. 12(a)–12(c). The non-zero kinetic energy density of the dynamic solution is shown in Fig. 12(d).

VI. DISCUSSION

Axial and helical symmetries are approximately present in various natural phenomena and laboratory settings, including fluid and plasma flows (see, e.g., Refs. 8, 9, 29, 30, 36 and references therein for reviews). In this paper, new exact explicit physical equilibrium solutions to the system of MHD equations (1.1) were found in the classical axial and helical symmetry reductions.

For the axially symmetric static equilibrium invariance reduction (Sec. III), the introduction of the potential with the meaning of a magnetic flux function reduces the model to a single PDE, the Grad–Shafranov equation (2.8). The arbitrary functions $P(\psi)$ and $I(\psi)$ defining the pressure and the poloidal magnetic field can be chosen so that the Grad–Shafranov equation linearizes. Separation of variables was used to find new solutions in terms of special functions; these solutions generalize the well-known family obtained in Ref. 8 (see also Ref. 30). Two separate families of solutions arose, depending on the type of pressure configuration chosen. For the case in which the plasma is surrounded by an ambient medium, the radial solution component (3.8) is generally written in terms of Whittaker functions. Depending on the parameter δ (3.7), physical solutions may be globally defined or restricted to a bounded domain with suitable boundary conditions (2.6). Explicit examples are presented in Sec. III A. The second family of solutions for the axially symmetric case has the radial component written in terms of Coulomb wave functions (Sec. III B). Solutions of this type are given by (3.17) and (3.18). Sample representatives of this new solution family,
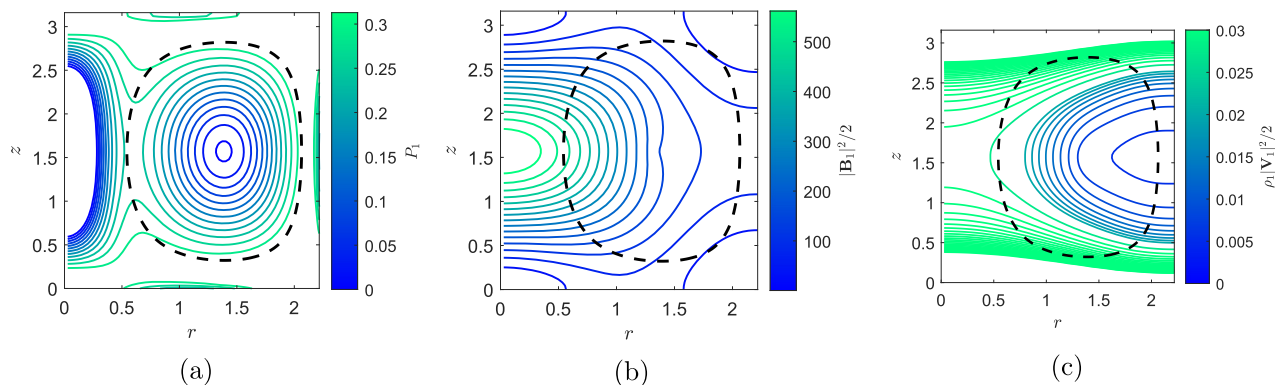

FIG. 11. The dynamic axially symmetric plasma equilibrium solution (5.3) and (5.5) corresponding to the static equilibrium solution shown in Fig. 2 above. (a) Pressure, (b) magnetic energy density, and (c) kinetic energy density. The dashed line shows the magnetic surface corresponding to the plasma domain boundary [see Fig. 2(a)].
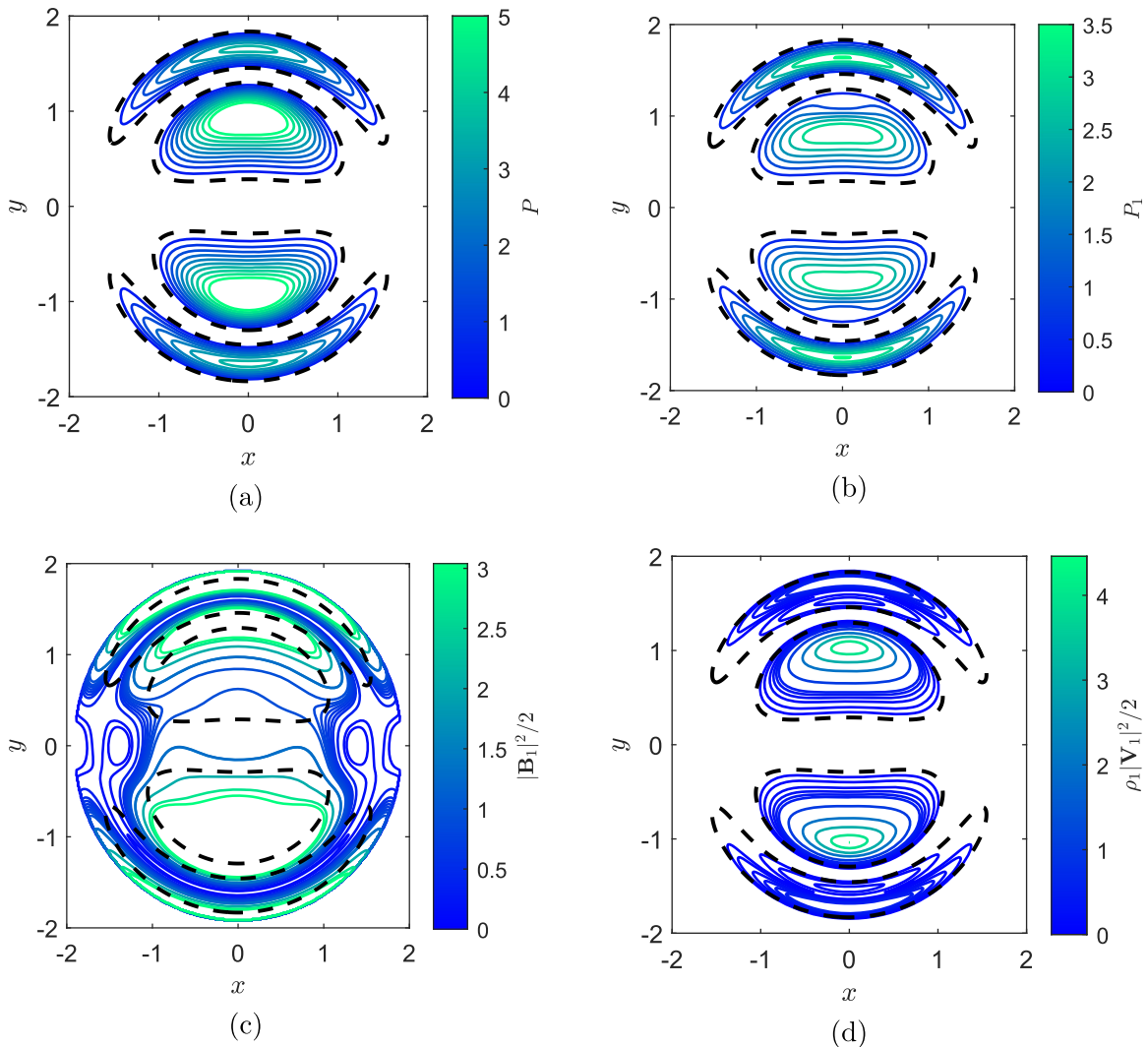
FIG. 12. (a) The (x, y)-cross section of the helical magnetic surfaces and contours of the pressure P, for the sample helically invariant static plasma equilibrium solution in Sec. IV B 1. (b) The transformed pressure P_1, obtained from Galas–Bogoyavlenskij transformations (5.3) with (5.7). (c) The cross sections of the transformed magnetic energy density. (d) The cross sections of the kinetic energy density in the transformed dynamic plasma equilibrium. The dashed line shows the magnetic surface corresponding to the plasma domain boundary [see Fig. 10(a)].

featuring the positive pressure profile (higher pressure toward the toroidal axis), are presented in Sec. III B 1.

For the helically invariant case (Sec. IV), the potential flux function $\psi(r, \xi)$ satisfies the JFKO equation (2.17) (which reduces to the Grad–Shafranov equation in the limit of the vanishing helical pitch). Similarly to the axial case, a linear version of the JFKO equation can be solved using separation of variables; the latter can be combined to form a rather general class. Two different families of solutions arise depending on the type of pressure configuration. For plasmas confined in an ambient medium (Sec. IV A), the flux function is found in terms of the confluent Heun function of a real argument; yields physically meaningful magnetic field profiles (see Sec. IV A 1). For certain special relations between solution parameters, Heun functions reduce to polynomials; this is the case obtained in terms of a decaying exponential and polynomials [formula (2.19)]. This subfamily of global solutions was obtained by Bogoyavlenskij.[9]

In Sec. V, Galas–Bogoyavlenskij transformations (5.1) and (5.3) were applied to the new axially and helically symmetric static MHD equilibria obtained earlier to yield exact field-aligned MHD equilibrium solutions with nonzero velocity: $\mathbf{V}_1 \| \mathbf{B}_1$. Such dynamic configurations share the set of magnetic surfaces with the original static solutions and involve two arbitrary functions (5.2). In particular, the plasma density ρ constant on magnetic surfaces is arbitrary for the static MHD system and is transformed into arbitrary density ρ_1 also constant on the magnetic surfaces.

06 February 2024 19:55:52

It is well known from laboratory experiments that plasmas have demonstrated a variety of instabilities (see, e.g., Ref. 2 and references therein for a review). An important question that concerns any exact plasma equilibria is, therefore, their stability with respect to various types of perturbations. A general result of Friedlander and Vishik[41] concerns the instability of non-field-aligned equilibria. Ilin and Vladimirov[42] state that Galas–Bogoyavlenskij transformations do not introduce new plasma instabilities (see also Ref. 43 for results on the stability of plasmas with current-vortex sheets). For each exact static plasma equilibrium solution, including those obtained above, it is, therefore, important to study its stability with respect to various perturbations. In particular, one can consider, analytically and/or numerically, the full time-dependent MHD system (1.1) written in helical coordinates, that is, system (B1) (see Appendix B). The dynamics of small perturbations is governed by solutions of the linearization of (B1) near a given static helically symmetric equilibrium defined by $\mathbf{V} = \partial/\partial\eta = 0$. A related question is the question of choice of arbitrary functions (5.2) in Galas–Bogoyavlenskij transformations that would corresponds to, for example, the smallest total energy of the resulting plasma configuration. The total energy density is given by $e = P + \rho|\mathbf{V}|^2/2 + |\mathbf{B}|^2/2\mu$; it is neither preserved by Galas–Bogoyavlenskij transformations [cf. (5.4)] nor is constant on magnetic surfaces. It would be of interest to develop a version of a variational principle that would help calculate "optimal" energy-minimizing forms of $F_1(\psi)$ and $F_2(\psi)$.

A long-term strategic direction is computation and application of exact and approximate solutions appropriate for the description of plasmas in complex geometries of various experimental settings that lack basic geometrical symmetries, such as stellarators and tokamaks, using, for example, the approximate symmetry approach (see, e.g., Ref. 44 and references therein). Approximate symmetries, such as quasiaxial and qualihelical symmetry in toroidal geometry,[45] manifest themselves in multiple plasma physics settings (e.g., Ref. 46).

In further work, it is also of interest to study the MHD system in the Dierkes and Oberlack's new time-dependent helical coordinates.[24]

ACKNOWLEDGMENTS

AUTHOR DECLARATIONS
Conflict of Interest

The authors have no conflicts to disclose.

Author Contributions

Jason Keller: Formal analysis (lead); Investigation (lead); Methodology (equal); Software (lead); Validation (equal); Visualization (lead); Writing – original draft (lead); Writing – review & editing (supporting). **Alexei Cheviakov:** Conceptualization (lead); Formal analysis (supporting); Funding acquisition (lead); Project administration (lead); Supervision (lead); Writing – original draft (supporting); Writing – review & editing (lead).

DATA AVAILABILITY

Data sharing is not applicable to this article as no new data were created or analyzed in this study.

APPENDIX A: THE BEHAVIOR OF AXIALLY SYMMETRIC SOLUTIONS OF THE FIRST FAMILY

Let us consider the radial part of the first family of axially symmetric separated solutions (3.8) (Sec. III A). When $\delta \notin \mathbb{N}$, the two radial solution components have the following asymptotic behavior.[47] First, when $r \to 0^+$, one has[47]

$$W_W\left(\kappa, \frac{1}{2}, qr^2\right) \sim \frac{1}{\Gamma(1-\delta)}.$$

Second, as $r \to \infty$, the other radial solution component diverges, behaving like

$$W_M(\delta, 1/2, qr^2) \sim \frac{\Gamma(2)}{\Gamma(1-\delta)} e^{\frac{qr^2}{2}}(qr^2)^{-\delta} \to \infty.$$

It follows that the poloidal magnetic field component $B^\varphi(r,z) = I(\psi)/r = \alpha\psi/r$ is singular both on the z-axis and at infinity, and the corresponding plasma equilibria solutions must be considered in domains bordered by magnetic surfaces that are bounded and separated from zero in the radial direction.

In the case when $\delta \in \mathbb{N}$, the functions $W_M(\delta, 1/2, qr^2)$ and $W_W(\delta, 1/2, qr^2)$ become linearly dependent and behave like

$$W_M(\delta, 1/2, qr^2) \sim W_W(\delta, 1/2, qr^2) \sim r^2 e^{\left(-\frac{qr^2}{2}\right)} L_{\delta-1}^{(1)}(qr^2), \quad \text{(A1)}$$

where $L_n^{(a)}(x)$ denote the Laguerre functions; in particular, $L_{\delta-1}^{(1)}(x)$ are polynomials of order $\delta - 1$. Using (2.9), one observes that B^φ and B^r which behave like $re^{\left(-\frac{qr^2}{2}\right)} L_{\delta-1}(qr^2)$ in the r variable are smooth, finite in the interval $0 \le r < \infty$, and go to zero for $r \to \infty$. Therefore, finite magnetic energy will be the case with these components. For the last component, $B^z = -\psi_r/r$ in (2.7) and (2.9), it is easy to observe as well that B^z remains finite for $0 \le r \le \infty$. From the form of the components of $\mathbf{B}$ in terms of (A1), it follows that the magnetic energy integral

$$\int_{\mathcal{U}} |\mathbf{B}(\mathbf{x})|^2 \, d^3x,$$

computed in a slab $\mathcal{U}$ defined by $z_1 \le z \le z_2$, $0 \le r < \infty$ is finite.

APPENDIX B: DYNAMIC MHD EQUATIONS IN HELICAL COORDINATES

We now explicitly write the full time-dependent system (1.1) of MHD equations in helical coordinates. Using the coordinate forms (2.14) in the basis (2.13) and the coordinate transformation (2.12), one arrives at the following PDEs. As before, subscripts denote partial derivatives.

- The continuity equation $\rho_t + \text{div } \rho\mathbf{V} = 0$

$$\rho_t + \rho_r V^r + \frac{1}{rQ}(\rho_\eta V^\eta + r\rho_\xi V^\xi) = 0. \quad \text{(B1a)}$$

- The incompressibility condition $\text{div } \mathbf{V} = 0$

$$(rV^r)_r + \frac{1}{Q}((V^\eta)_\eta + r(V^\xi)_\xi) = 0. \quad \text{(B1b)}$$

- The absence of magnetic charges div $\mathbf{B} = 0$

$$(rB^r)_r + \frac{1}{Q}((B^\eta)_\eta + r(B^\xi)_\xi) = 0. \tag{B1c}$$

- The momentum equations (1.1b)

$$(V^r)_t = \frac{1}{\rho r^3 Q}\left(-r^3 Q'((B^\eta)^2 + (B^\xi)^2)\right.$$
$$+ Q^3(2r\gamma(B^\eta B^\xi - \rho V^\eta V^\xi) + \gamma^2 \rho (V^\xi)^2)$$
$$+ Q(r^2(B^\eta)^2 - r^3(\rho V^r(V^r)_r + B^\eta(B^\eta)_r + B^\xi(B^\xi)_r + P_r))$$
$$\left. + r^3((B^r)_\xi B^\xi - \rho(V^r)_\xi V^\xi) + r^2((B^r)_\eta B^\eta - \rho(V^r)_\eta V^\eta)\right), \tag{B1d}$$

$$(V^\eta)_t = \frac{1}{\rho r Q}\left((rQ' + 2Q^3 - Q)(B^r B^\eta - \rho V^r V^\eta)\right.$$
$$+ rQ(B^r(B^\eta)_r - \rho V^r(V^\eta)_r)$$
$$+ r((B^\eta)_\xi B^\xi - \rho(V^\eta)_\xi V^\xi) - (B^r(B^r)_\eta$$
$$\left. + B^\xi(B^\xi)_\eta + \rho V^\eta(V^\eta)_\eta + P_\eta)\right), \tag{B1e}$$

$$(V^\xi)_t = \frac{1}{\rho r^2 Q}\left(r^2 Q'(B^r B^\xi - \rho V^r V^\xi)\right.$$
$$- 2\gamma Q^3(B^r B^\eta - \rho V^r V^\eta) + r^2 Q(B^r(B^\xi)_r - \rho V^r(V^\xi)_r)$$
$$- r^2(B^r(B^r)_\xi + B^\eta(B^\eta)_\xi + \rho V^\xi(V^\xi)_\xi + P_\xi)$$
$$\left. + r(B^\eta(B^\xi)_\eta - \rho V^\eta(V^\xi)_\eta)\right). \tag{B1f}$$

- The magnetic field evolution equations (1.1c)

$$(B^r)_t = \frac{1}{Q}(V^r B^\xi - B^r V^\xi)_\xi + \frac{1}{rQ}(V^r B^\eta - V^\eta B^r)_\eta, \tag{B1g}$$

$$(B^\eta)_t = \frac{2\gamma Q^2}{r^2}(V^\xi B^r - V^r B^\xi) + \frac{1}{Q}(Q(V^\eta B^r - V^r B^\eta))_r$$
$$+ \frac{1}{Q}(V^\eta B^\xi - V^\xi B^\eta)_\xi, \tag{B1h}$$

$$(B^\xi)_t = \frac{2Q^2}{r}(V^\xi B^r - B^\xi V^r) + \frac{r}{Q}\left(\frac{Q}{r}(V^\xi B^r - V^r B^\xi)\right)_r$$
$$+ \frac{1}{rQ}(V^\xi B^\eta - V^\eta B^\xi)_\eta. \tag{B1i}$$

It is straightforward to verify that when $\mathbf{B} = \partial/\partial\eta = 0$, the PDEs reduce to helically invariant Euler equations and coincide with Eq. (2.9) of Ref. 23 ($\nu = 0$).

REFERENCES

[1] A. F. Cheviakov, "Construction of exact plasma equilibrium solutions with different geometries," Phys. Rev. Lett. **94**(16), 165001 (2005).
[2] A. F. Cheviakov, *Symmetries and Exact Solutions of Plasma Equilibrium Equations* (Queen's University Press, 2004).
[3] A. Ferrari, "Modeling extragalactic jets," Annu. Rev. Astron. Astrophys. **36**(1), 539–598 (1998).
[4] J. H. Beall, "A review of astrophysical jets," Acta Polytech. CTU Proc. **1**(1), 259–264 (2014).
[5] D. C. Hines, F. N. Owen, and J. A. Eilek, "Filaments in the radio lobes of M87," Astrophys. J. **347**, 713–726 (1989).
[6] M. Hardcastle, D. Worrall, R. Kraft, W. Forman, C. Jones, and S. Murray, "Radio and X-ray observations of the jet in Centaurus A," Astrophys. J. **593**(1), 169 (2003).
[7] R. Blandford and D. Payne, "Hydromagnetic flows from accretion discs and the production of radio jets," Mon. Not. R. Astron. Soc. **199**(4), 883–903 (1982).
[8] O. I. Bogoyavlenskij, "Astrophysical jets as exact plasma equilibria," Phys. Rev. Lett. **84**(9), 1914 (2000).
[9] O. I. Bogoyavlenskij, "Helically symmetric astrophysical jets," Phys. Rev. E **62**(6), 8616 (2000).
[10] P. Moon and D. E. Spencer, *Field Theory Handbook: Including Coordinate Systems, Differential Equations and Their Solutions* (Springer-Verlag, 1971).
[11] T. Sarpkaya, "On stationary and travelling vortex breakdowns," J. Fluid Mech. **45**(3), 545–559 (1971).
[12] S. Wang, "Theory of tokamak equilibria with central current density reversal," Phys. Rev. Lett. **93**, 155007 (2004).
[13] S. You, G. Yun, and P. Bellan, "Dynamic and stagnating plasma flow leading to magnetic-flux-tube collimation," Phys. Rev. Lett. **95**(4), 045002 (2005).
[14] A. Gupta and R. Kumar, "Three-dimensional turbulent swirling flow in a cylinder: Experiments and computations," Int. J. Heat Fluid Flow **28**(2), 249–261 (2007).
[15] I. Satoru, "An experimental study on extinction and stability of tubular flames," Combust. Flame **75**(3–4), 367–379 (1989).
[16] L. Vermeer, J. Sorensen, and A. Crespo, "Wind turbine wake aerodynamics," Prog. Aerosp. Sci. **39**(6–7), 467–510 (2003).
[17] A. Mitchell, S. Morton, and J. Forsythe, "Wind turbine wake aerodynamics," Air Force Academy Colorado Springs, Department of Aeronautics, Report No. ADA425027, 1997.
[18] S. Alekseenko, P. Kuibin, V. Okulov, and S. Shtork, "Helical vortices in swirl flow," J. Fluid Mech. **382**, 195–243 (1999).
[19] S. Alekseenko and V. Okulov, "Swirl flow in technical applications (review)," Thermophys. Aeromech. **3**, 97–128 (1996).
[20] J. Kubitschek and P. Weidman, "Helical instability of a rotating liquid jet," Phys. Fluids **20**(9), 091104 (2008).
[21] M. Frewer, M. Oberlack, and S. Guenther, "Symmetry investigations on the incompressible stationary axisymmetric Euler equations with swirl," Fluid Dyn. Res. **39**(8), 647–664 (2007).
[22] A. F. Cheviakov and G. W. Bluman, "On locally and nonlocally related potential systems," J. Math. Phys. **51**(7), 073502 (2010).
[23] O. Kelbin, A. F. Cheviakov, and M. Oberlack, "New conservation laws of helically symmetric, plane and rotationally symmetric viscous and inviscid flows," J. Fluid Mech. **721**, 340–366 (2013).
[24] D. Dierkes and M. Oberlack, "Euler and Navier–Stokes equations in a new time-dependent helically symmetric system: Derivation of the fundamental system and new conservation laws," J. Fluid Mech. **818**, 344–365 (2017).
[25] S. L. Bragg and W. R. Hawthorne, "Some exact solutions of the flow through annular cascade actuator discs," J. Aeronaut. Sci. **17**(4), 243–249 (1950).
[26] H. Grad and H. Rubin, "Hydromagnetic equilibria and force-free fields," J. Nucl. Energy **7**(3–4), 284–285 (1958).
[27] V. Shafranov, "On magnetohydrodynamical equilibrium configurations," Sov. Phys. JETP **6**(3), 1013 (1958).
[28] J. L. Johnson, C. Oberman, R. Kulsrud, and E. Frieman, "Some stable hydromagnetic equilibria," Phys. Fluids **1**(4), 281–296 (1958).
[29] R. Kaiser and D. Lortz, "Ball lightning as an example of a magnetohydrodynamic equilibrium," Phys. Rev. E **52**(3), 3034 (1995).
[30] C. Atanasiu, S. Günter, K. Lackner, and I. Miron, "Analytical solutions to the Grad–Shafranov equation," Phys. Plasmas **11**(7), 3510–3518 (2004).
[31] P. Alexandroff and H. Hopf, *Topologie* (Springer Verlag, 1974), Vol. 1.
[32] O. I. Bogoyavlenskij, "Infinite symmetries of the ideal MHD equilibrium equations," Phys. Lett. A **291**(4–5), 256–264 (2001).
[33] R. Lüst and A. Schlüter, "Axialsymmetrische magnetohydrodynamische gleichgewichtskonfigurationen," Z. Naturforsch., A **12**(10), 850–854 (1957).
[34] M. J. M. Hill, "VI. On a spherical vortex," Philos. Trans. R. Soc. London, Ser. A **185**, 213–245 (1894).
[35] P. J. Olver, *Applications of Lie Groups to Differential Equations* (Springer Verlag, 2000), Vol. 107.
[36] D. Dierkes, A. Cheviakov, and M. Oberlack, "New similarity reductions and exact solutions for helically symmetric viscous flows," Phys. Fluids **32**(5), 053604 (2020).

[37]N. Saad, "On the solvability of confluent Heun equation and associated orthogonal polynomials," arXiv:1509.00090 (2015).

[38]F. Galas, "Generalized symmetries for the ideal MHD equations," Physica D **63**(1–2), 87–98 (1993).

[39]O. I. Bogoyavlenskij, "Symmetry transforms for ideal magnetohydrodynamics equilibria," Phys. Rev. E **66**(5), 056410 (2002).

[40]A. F. Cheviakov, "Bogoyavlenskij symmetries of ideal MHD equilibria as Lie point transformations," Phys. Lett. A **321**(1), 34–49 (2004).

[41]S. Friedlander and M. M. Vishik, "On stability and instability criteria for magnetohydrodynamics," Chaos **5**(2), 416–423 (1995).

[42]K. Ilin and V. Vladimirov, "Energy principle for magnetohydrodynamic flows and Bogoyavlenskij's transformation," Phys. Plasmas **11**(7), 3586–3594 (2004).

[43]K. Ilin, Y. Trakhinin, and V. A. Vladimirov, "The stability of steady magnetohydrodynamic flows with current-vortex sheets," Phys. Plasmas **10**(7), 2649–2658 (2003).

[44]M. R. Tarayrah, B. Pitzel, and A. Cheviakov, "Two approximate symmetry frameworks for nonlinear partial differential equations with a small parameter: Comparisons, relations, approximate solutions," Eur. J. Appl. Math. **34**(5), 1017–1045 (2023).

[45]M. Landreman and E. Paul, "Magnetic fields with precise quasisymmetry for plasma confinement," Phys. Rev. Lett. **128**(3), 035001 (2022).

[46]A. Enciso, A. Luque, and D. Peralta-Salas, "MHD equilibria with nonconstant pressure in nondegenerate toroidal domains," arXiv:2104.08149 (2021).

[47]See http://dlmf.nist.gov/ for "NIST Digital Library of Mathematical Functions"; accessed 15 March 2020.

06 February 2024 19:55:52